Orientation Estimation using Differences in WiFi Signal Behavior in LOS and NLOS Cases

Jiaqing Yang*§, Kota Tsubouchi†§, Shoma Nakamae*, and Nobuhiko Nishio*
* Ritsumeikan University, Shiga, JAPAN
Email: {yang, andy, nishio}@ubi.cs.ritsumei.ac.jp
†LY Corporation, Tokyo, JAPAN
Email: ktsubouc@yahoo-corp.jp

2024 IEEE International Conference on Pervasive Computing and Communications Workshops and other Affiliated Events (PerCom Workshops) | 979-8-3503-0436-7/24/$31.00 ©2024 IEEE | DOI: 10.1109/PerComWorkshops59983.2024.10502827

***Abstract*—Accurate orientation information is essential for calibrating pedestrian dead reckoning (PDR) systems, which determine a user's position based on accelerometer and gyroscope data. Calibrating PDR helps mitigate cumulative errors during navigation, but previous methods have struggled to correct errors in body rotation direction using gyro sensors. Traditional approaches, such as magnetic compasses, are impractical indoors due to interference. Instead, this paper proposes a unique technique that uses readily available smartphone data—Received Signal Strength Indicator (RSSI) and Round-Trip-Time (RTT)-based distance measurements. The core principle is that RSSI is influenced by obstacles and user presence (non-line-of-sight or NLOS conditions), while RTT-based distances remain more stable. By accurately measuring distances and estimating expected signal strengths, the method distinguishes between line-of-sight (LOS) and NLOS conditions. Field tests confirm the method's efficacy, achieving a remarkable 90% accuracy in estimating WiFi-AP direction. This innovative approach contributes to addressing cumulative errors in smartphone-based navigation without relying on specialized equipment.**

***Index Terms*—Orientation Estimation, Wi-Fi, LOS, NLOS, RTT**

I. Introduction

This paper proposes a technique for estimating which direction a user holding a smartphone is facing relative to a single wifi access point.

Estimating the user's orientation relative to the access point would be useful for calibrating the orientation of the PDR. PDR is a technique to locate the user's position by accumulating the amount of progress and change in direction due to acceleration and gyro. However, the cumulative error is an issue, and the cumulative error is reset by calibrating the system with indoor positioning using wifi or check-in information. There are many techniques to calibrate the location of the user and the stride length per step, but to best of our knowledge, there is no way to reset the cumulative error for the direction of body rotation using a gyro sensor. A simple method would be to use a magnetic compass to compensate for this, but this is unlikely to be used in navigation indoors, as the correct direction cannot be estimated by vending machines, digital signage, etc [1], [2].

Therefore, we propose a completely new technique to estimate the user's body orientation to a wifi AP without using information from other sensors. In general, it is well known that the user's orientation to the AP can be supplemented by CSI. However, wifi-CSI information requires the use of dedicated terminals and measurement devices, and cannot be measured by general-purpose smartphones. We have found that two types of information obtained from wifi that can be measured with commercially available smartphones can be used to estimate the user's body orientation relative to the AP: RSSI (radio wave strength) and RTT-based distance measurement data.

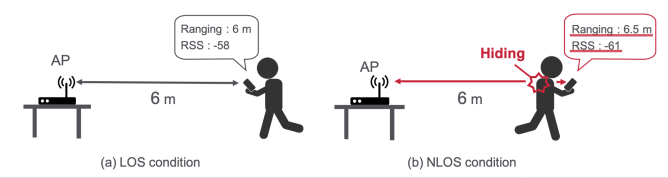

Fig. 1: Distance between device and AP estimated using RSSI differs between LOS and NLOS cases; for RTT they are nearly equal.

The proposed technique is based on the principle that RSSI is affected, but the ranging results using RTT are not, when there is an obstacle between the smartphone and the wifi-AP (NLOS). The RSSI is reduced by the absorption of radio waves by the user's body in NLOS, while the RTT is almost unaffected and conveys the correct ranging results by measuring the correct distance between the AP and the user and estimating the expected radio wave strength at that distance. This principle is that by measuring the correct distance relationship between the AP and the user and estimating the expected signal strength at that distance, it is possible to estimate whether the AP is in LOS or NLOS. A specific example to illustrate the key idea in more detail is shown in Figure1. In the example in the figure, when the user is facing backward and the body is an obstacle and in NLOS, the distance between the smartphone and the AP estimated from RSSI is 6.5 m, 0.5 m longer than actual. However, when the distance is measured using Wifi-RTT, the distance remains at 6m and is almost unaffected. The key idea of this study is to use this difference to determine LOS and NLOS.

To verify the effectiveness of the proposed technique, we carried out a field test. As a result, it was found that the

§These two authors contribute equally to the work.

direction estimation for wifi-APs can be achieved with high accuracy of about 90%. The contributions of this research are as follows.

- We found that the difference in the characteristics of RSSI and RTT ranging results in the NLOS state can be used to estimate the direction of the user toward the wifi-AP.
- The results of actual data acquisition and validation showed that the estimation accuracy was more than 90%.

II. Related Works

A. Pedestrian Dead Reckoning (PDR)

PDR is a technique used to estimate a user's position by utilizing a smartphone's accelerometer and gyro sensors [3]. With an initial position and direction provided, PDR accumulates the amount of progress and change in direction from these sensors to determine the user's location. One of the advantages of PDR is that it doesn't rely on external infrastructure, as it solely utilizes the smartphone's sensors. However, it does suffer from the issue of cumulative errors, as it estimates the user's position relative to the initial position and direction. As the walking distance increases, accumulated errors become more pronounced [4].

B. Accumulated Error Offset for PDR

To mitigate the cumulative error of PDR, various techniques have been employed, such as indoor positioning with WiFi [5]–[9] and the utilization of anchor points [10]–[13]. Sun et al. [14] proposed a position model based on the Extended Kalman Filter (EKF) algorithm that fuses WiFi and PDR, resulting in an approximately 10% to 20% improvement in positioning accuracy compared to PDR alone. Chattha et al. [15] detected events related to using elevators and escalators, and employed map information to reset the cumulative error of PDR. In addition to these methods using absolute position information, there are techniques aimed at reducing the cumulative error by calibrating step length [16]–[20]. Yao et al. [21] recognized three walking patterns (Normal Walk, March in Place, and Quick Walk) using smartphones and estimated step length based on the recognition results. While these techniques successfully mitigated the cumulative error in positioning results, but to the best of our knowledge, there is currently no method to reset the cumulative error in the direction of body rotation using a gyro sensor.

C. Channel State Information (CSI)

CSI which is much finer-grained than RSS has attracted attention and various applications, such as positioning and gesture recognition, was proposed. Some direction estimation method using CSI was also proposed. Wu et al. [22] proposed a method which can track moving distance, heading direction by using only one AP. Also, some researchers proposed CSI-based device-free direction estimation [23], [24]. These methods can estimate the direction with high accuracy even in multi-path rich area. A CSI tools were also developed [25], [26], but most devices do not support this yet. Therefore, it is not realistic to use the CSI-based direction estimation method.

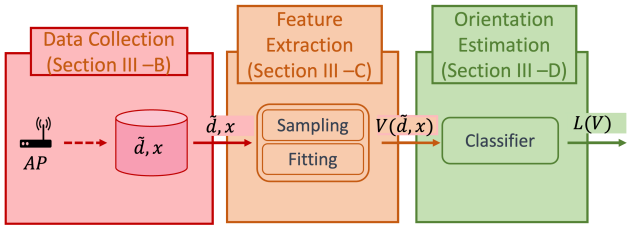

Fig. 2: Flow of the proposed approach

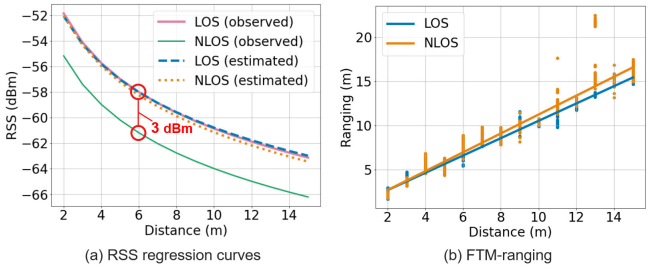

Fig. 3: RSSI/RTT-ranging changes between LOS and NLOS: distance estimation by RSSI is affected, but distance estimation by RTT is not in NLOS case.

D. Wifi Round Trip Time (Wifi-RTT)

Wifi-RTT is a standardized distance measurement protocol that was introduced in 2016 under the IEEE 802.11mc standard [27]. It leverages the Time of Flight (ToF) of wifi radio wave to measure the distance between wifi-AP and mobile devices. Due to its standardization, it is now relatively easy to procure base stations that support Wifi-RTT. Furthermore, in 2018, Google introduced support for Wifi-RTT in the Android Pie smartphone operating system [28], making Wifi-RTT accessible on commercially available smartphones. For these reasons, we believe that Wifi-RTT is more accessible and practical compared to CSI, as it doesn't require dedicated terminals or devices. In this research, we propose a direction estimation method that can be generally applied using Wifi-RTT.

III. Approach

The proposed approach in this research estimates the user's orientation relative to a wifi-AP by utilizing the difference in characteristics between RSSI and RTT ranging in the NLOS. Figure 2 shows the flow of the proposed approach, which is divided into three phases. First, we collected the data from the wifi-AP using a smartphone. Second, we conducted sampling and fitting on the collected data to extract feature vectors. Finally, we estimated the user's body orientation relative to the wifi-AP by using the extracted features vectors.

A. Difference in characteristics between RSSI and RTT ranging in the NLOS

When the user's body is located between smartphone and wifi-AP (i.e.,the case of NLOS), there are difference in the changes observed in the RSSI and RTT-ranging results. In the

NLOS, the user's body absorbs the wifi radio signal, leading to a reduction in RSSI. On the other hand, RTT is minimally affected and provides accurate ranging results.

To verify this phenomenon, we conducted preliminary experiments in an $11\ \mathrm{m} \times 16\ \mathrm{m}$ room. In the room, a Google Wi-Fi was set up as the wifi-AP, and a Pixel 3a as the smartphone. An observer collected data at $1\ \mathrm{m}$ intervals from $2\ \mathrm{m}$ to $15\ \mathrm{m}$ away from wifi-AP while holding the smartphone in front of the chest. Figure 3(a) depicts the wifi signal sensing results in the case of both LOS and NLOS, with a $3\ \mathrm{dBm}$ difference between them. In Figure 3(b), RTT ranging results for both LOS and NLOS conditions are displayed. In the NLOS, RTT ranging errors gradually expanded from $6\ \mathrm{m}$ to slightly over $0.5\ \mathrm{m}$.

These results demonstrate that RSSI and RTT ranging results differ in LOS and NLOS. However, since RSSI and RTT ranging results have different units, a direct comparison is challenging. In other words, it's not feasible to effectively illustrate the difference in characteristics between RSSI and RTT ranging in the NLOS. To resolve this issue, Equation. 1 is employed to calculate the estimated RSSI as $F(d)$.

$$F(d) = a \cdot \log_{10}(d) + b, \tag{1}$$

where, d represents the distance from the wifi-AP. a and b are parameters derived from observed RSSI and RTT ranging results in the LOS. By substituting RTT ranging results into d, the estimated RSSI can be calculated, as represented by the dotted line in Figure 3(a). As evident in Figure 3(a), while there is a significant difference in observed RSSI between LOS and NLOS, the estimated RSSI remains relatively constant. In other words, the difference between estimated RSSI and observed RSSI in the NLOS is more pronounced compared to the LOS. This research capitalizes on this phenomenon to differentiate between LOS and NLOS, and additionally, to estimate the user's body orientation relative to the wifi-AP.

B. Data Collection

In the environment where Wifi-AP is deployed, raw data $\{\hat{d}, x\}$ is collected using a smartphone. $\hat{d}$ represents the RTT ranging result, and x corresponds to RSSI value. It's important to note that the RTT ranging result differs from the actual distance, necessitating calibration as follows:

$$\tilde{d} = \hat{d} + \phi, \tag{2}$$

where, ϕ represents the offset determined by the kind of wifi-AP and the smartphone because the offset depends on hardware clock frequency. The data is stored in the smartphone's memory, to be harnessed during the process of feature extraction via sampling. Furthermore, these data are labeled with the ID of the wifi-AP.

C. Feature Extraction

The phase of feature extraction comprises two fundamental steps: Sampling and Fitting. In this section, we will explain how the feature vectors were extracted from the data by Sampling and Fitting. Furthermore, we will shall expound how the extracted feature vectors work to orientation estimation.

1) Sampling: In the sampling step, the mean and standard deviation of the RSSI and RTT ranging results are calculated. The RSSI and RTT ranging results exhibit significant outliers, especially in the NLOS. Furthermore, this variability in RSSI and RTT ranging results increases as the distance from the wifi-AP grows, particularly in the NLOS. To mitigate the impact of such outliers, sampling is conducted using data from the most recent s observations, and four feature vectors were extracted from these data: the mean $\mu^{\tilde{d}}$ and standard deviation $\sigma^{\tilde{d}}$ of the distance estimation results, and the mean μ^{x} and standard deviation σ^{x} of the RSSI. The sampling obeys the following equation:

$$S(\tilde{d}, x) = \{\mu^{\tilde{d}}, \sigma^{\tilde{d}}, \mu^{x}, \sigma^{x}\}. \tag{3}$$

2) Fitting: In the Fitting step, we extract the feature vector $D^{\mathrm{RSS}}\left(\mu^{(\tilde{d})}, \mu^{(x)}\right)$, which represents the difference between the mean of the observed RSSI and estimated RSSI from the mean of the ranging. The fitting model employs the same as Equation 1 in Section III-A, represented as $F\left(\mu^{(\tilde{d})}\right)$.The parameters a and b are chosen to minimize the difference between observed RSSI and estimated RSSI, as expressed in equation:

$$\underset{a,b}{} \sum_{j=0}^{N} \left(F\left(\mu_j^{(\tilde{d})}\right) - x_j\right)^2, \tag{4}$$

where, j represents the index of the training data, and N denotes the number of training data. As explained in Section III-A, the RTT ranging results is less likely to fluctuate compared with the RSSI in the NLOS. Therefore, the estimated RSSI through fitting tends to be larger than the observed RSSI. Consequently, the feature is calculated using the following equation:

$$D^{\mathrm{RSSI}}\left(\mu^{(\tilde{d})}, \mu^{(x)}\right) = F\left(\mu^{(\tilde{d})}\right) - \mu^{(x)}. \tag{5}$$

3) Feature Vectors: The feature vectors used for orientation estimation amount to a total of five. The first feature vector is the mean of RTT ranging results, denoted as $\mu^{(\tilde{d})}$. This is utilized to effectively learn observed values that vary based on the distance from the wifi-AP. The second feature vector is the standard deviation of RTT ranging results, denoted as $\sigma^{(\tilde{d})}$. This is employed to account for the significant variation in measured distances, particularly in the NLOS.The third feature vector is the standard deviation of RSSI, denoted as $\sigma^{(x)}$. This is almost same for each class but improves classification accuracy. The fourth feature vector is the difference between observed RSSI and estimated RSSI, represented as $D^{\mathrm{RSSI}}\left(\mu^{(\tilde{d})}, \mu^{(x)}\right)$. As explained in Section III-A, this value is crucial. The fifth feature vector is the difference between RTT ranging results and actual distance, denoted as $D^{\mathrm{RTT}}\left(\mu^{(\tilde{d})}, d\right)$. The utilization of this feature is aimed at accounting for the varying RTT ranging results in the NLOS. The feature vector is derived as follows:

TABLE I: Orientation rang of each class

O	$\theta_{\min 1}$	$\theta_{\max 1}$	$\theta_{\min 2}$	$\theta_{\max 2}$
Front	$-\frac{3}{8}\pi$	$+\frac{3}{8}\pi$	-	-
Sides	$-\frac{5}{8}\pi$	$-\frac{3}{8}\pi$	$+\frac{3}{8}\pi$	$+\frac{5}{8}\pi$
Rear-sides	$-\frac{7}{8}\pi$	$-\frac{5}{8}\pi$	$+\frac{5}{8}\pi$	$+\frac{7}{8}\pi$
Rear	$-$	$-$	$+\frac{7}{8}\pi$	$+\frac{8}{8}\pi$

$$D^{\mathrm{RTT}}\left(\mu^{(\tilde{d})}, d\right) = \mu^{(\tilde{d})} - d, \tag{6}$$

where, the user's position is assumed to be known, and the actual distance, denoted as d, can be calculated based on the spatial relationship between the user's position and the wifi-AP. Therefore, the feature vector set for orientation estimation is presented as follows:

$$V\left(\tilde{d}, x\right) = \left\{\mu^{(\tilde{d})}, \sigma^{(\tilde{d})}, \sigma^{(x)}, D^{\mathrm{RSSI}}\left(\mu^{(\tilde{d})}, \mu^{(x)}\right), D^{\mathrm{RTT}}\left(\mu^{(\tilde{d})}, d\right)\right\}. \tag{7}$$

D. Orientation Estimation

1) Subdivision of the classes: In Section III-A, we discussed the principle of estimating LOS and NLOS using the difference between observed RSSI and estimated RSSI. However, representing the user's orientation towards the wifi-AP with just two classes, LOS and NLOS, is too broad when considering a full $360°$ range. For example, if a user is facing sideways relative to the wifi-AP, regardless of LOS or NLOS estimation, there could be an error of up to $90°$ in the actual orientation. To address this issue, further subdivision of the classes is necessary.

Here we reconsider the principle of estimating LOS and NLOS. In the case of NLOS, the user's body absorbs the wifi radio signal, causing a reduction in observed RSSI. However, the estimated RSSI from RTT ranging results is minimally affected. We are using the difference between these two values to estimate LOS and NLOS. In other words, based on the assumption that the user's orientation towards the wifi-AP affects observed RSSI, we can hypothesize that different user orientations lead to varying observed RSSI. Building on this hypothesis, we classify the user's body orientation relative to the wifi-AP into four classes: "Front" "Sides" "Rear-sides" and "Rear".

2) Building the Orientation Estimation Model: The Orientation Estimation Model employs a support vector machine as the classifier and learns to classify the four classes of angles as shown in TABLE I. We applied the RBF kernel to enable the learning of complex boundaries between classes and conducted feature normalization as a pre-processing step before training.

IV. EVALUATION

A. Experimental Conditions and Data Collection

To evaluate the orientation estimation accuracy, we conducted evaluation experiments in a room$(11\ \mathrm{m} \times 16\ \mathrm{m})$ located on the sixth floor of a building within our university's campus. The experimental environment is depicted in Figure 4. We set up a single Google Wi-Fi as the wifi-AP and used a Pixel 4a as the smartphone.

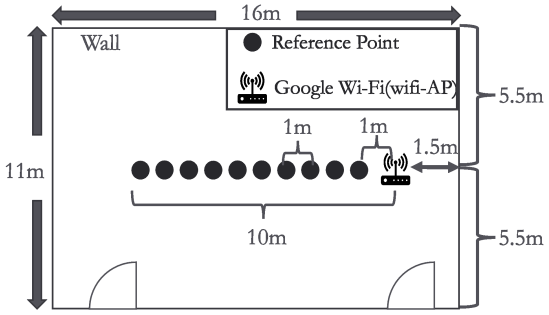

Fig. 4: Environment Overview

The observer performed data collection while holding the smartphone in front of their chest. We set up a total of 10 reference points at intervals of $1\ \mathrm{m}$ from $1\ \mathrm{m}$ to $10\ \mathrm{m}$ away from wifi-AP. At each reference point, the observer turned to eight different orientations and collected data for $2\ \mathrm{min}\ 30\ \mathrm{s}$. At a sampling rate of $6\ \mathrm{Hz}$, the final number of samples obtained was as follows:"Front" had 25433 samples, Sides had 16849 samples, Rear-sides had 16803 samples, and Rear had 8468 samples. The difference in the number of samples collected from each orientation can be attributed to the different definitions of each orientation's angles, as outlined in TABLEI. For instance, while angles within the range of $3/4\pi$ were defined as "Front","Rear" covers a $1/4\pi$ angle, making it one-third of the size compared to "Front". After collecting the data, it was shuffled, and then 70% of the data was used as the training data, while the remaining 30% was used as the test data.

B. Evaluation results

TABLE II displays the Confusion Matrix for Orientation Estimation method on the test data. While there are some misclassified samples, a significant portion of the samples are correctly classified. Note that since the method estimates all four directions simultaneously, this is a problem that is about 25% accurate for random selection.

Furthermore, to illustrate the performance of the Orientation Estimation method, precision, recall, and F-value were computed from the Confusion Matrix and are presented in TABLEIII. As evident from TABLEIII, the Orientation Estimation method exhibits high performance, achieving an accuracy of approximately 90% in estimating the observer's orientation relative to the wifi-AP. In particular, Front can be estimated with an accuracy of over 90%. Other orientations, while slightly less accurate than the Front, still achieve an accuracy of over 85%.

V. DISCUSSION

In this section, we further analyze and evaluate the experimental data from Section IV from different perspectives to discuss the validity of the class classification and the usefulness of the Orientation Estimation method.

TABLE II: Confusion Matrix for Orientation Estimation

		Predicted			
		Front	Sides	Rear-sides	Rear
Actual	Front	7189	382	261	62
	Sides	290	4458	315	217
	Rear-sides	166	206	4623	100
	Rear	39	175	140	2232

TABLE III: The classification accuracy of Orientation Estimation

	Precision	Recall	F-value
Front	0.94	0.91	0.92
Sides	0.85	0.84	0.85
Rear-sides	0.87	0.91	0.89
Rear	0.85	0.86	0.86
Average	0.88	0.88	0.88

A. *Validity of Class Classification*

Figure 5 displays the RSSI and RTT ranging results when the observer is 10 m away from the wifi-AP. From this figure, we observe the following characteristics concerning the user's orientation to the AP and the observed RSSI and RTT ranging results:

- **Front** : The ranging and the RSSI are not attenuated.
- **Sides** : The ranging is relatively not attenuated, but the RSSI is attenuated.
- **Rear-sides** : A slight positive bias occurs in the ranging, and the RSSI is also slightly attenuated.
- **Rear** : A positive bias occurs in the ranging, and the RSSI is also attenuated.

Furthermore, when the observer is facing directly toward the AP and when they are facing slightly to the left or right, the observed values are quite similar, making them indistinguishable.

Based on these observations, it is clear that classifying the user's orientation to the wifi-AP into four classes: "Front" "Sides" "Rear-sides" and "Rear" is a valid approach.

B. *The usefulness of the Orientation Estimation method*

Based on these observations, we can conclude that using our method and set up a single AP in an environment enables highly accurate directional estimation.

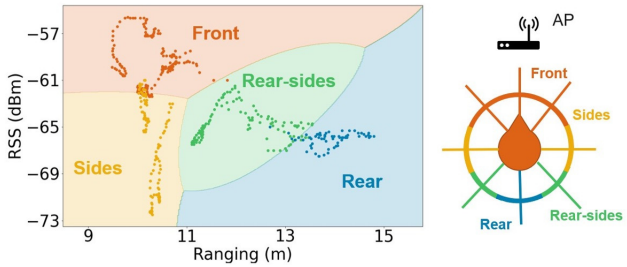

Fig. 5: RSSI and RTT ranging results 10 m apart from AP

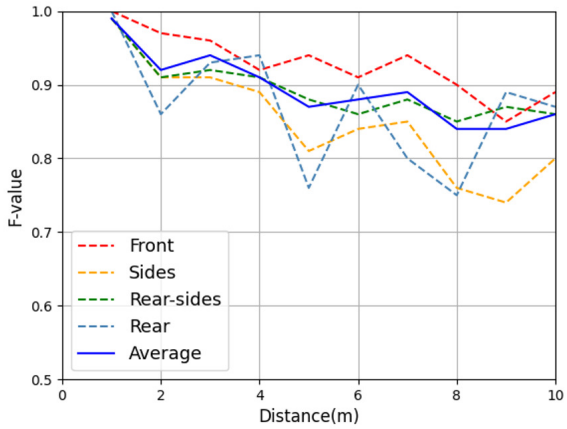

Fig. 6: The F-value for each reference point

Figure 6 represents the orientation estimation accuracy for each reference point. The horizontal axis in the figure represents the distance from the wifi-AP, while the vertical axis shows the F-value for each class of orientation estimation. From this figure, we can observe that as the distance from the wifi-AP increases, the classification accuracy for orientation estimation tends to decrease. This is likely due to what was explained in SectionIII-C1 where it was mentioned that the variation in RSSI and RTT ranging results increases as the distance from the wifi-AP grows. However, even at the reference point furthest from the wifi-AP (10 m), the average F-value for each orientation is still around 85%. Furthermore, when the distance from the wifi-AP is within 4 m, the average F-value for each direction is 90% or higher. Especially at the reference point 1 m from the wifi-AP, data collected from all directions achieve F-values of 99% or more, demonstrating highly accurate directional estimation.When used concurrently with PDR, the orientation estimation of PDR accumulates errors, leading to a degradation in accuracy. In contrast, our method ensures the stable and precise estimation of approximate orientation. Moreover, increasing in the number of wifi-AP enhances the precision of our method in orientation estimation, proving useful for calibrating the orientation of the PDR.

VI. Conclusion

We proposed a new technique to estimate the direction a user is facing toward a WiFi-AP using the difference in behavior between WiFi-RTT and RSSI during NLOS. Specifically, the idea is to estimate the direction based on the finding that NLOS is more likely when there is a difference between the distance estimated from RSSI and the distance estimated from WiFi-RTT. We demonstrated that the results of the demonstration show that the estimation can be done with an overall performance of more than 80% accuracy, including the condition of looking sideways as well as forward and backward. This novel method is expected to play a significant role in rectifying cumulative errors in smartphone-based navigation without the need for specialized hardware.

REFERENCES

[1] J. Chung, M. Donahoe, C. Schmandt, I.-J. Kim, P. Razavai, and M. Wiseman, "Indoor location sensing using geo-magnetism," in *Proceedings of the 9th international conference on Mobile systems, applications, and services*, 2011, pp. 141–154.

[2] B. Li, T. Gallagher, A. G. Dempster, and C. Rizos, "How feasible is the use of magnetic field alone for indoor positioning?" in *2012 International Conference on Indoor Positioning and Indoor Navigation (IPIN)*, 2012, pp. 1–9.

[3] P. D. Groves, "Navigation using inertial sensors [tutorial]," *IEEE Aerospace and Electronic Systems Magazine*, vol. 30, no. 2, pp. 42–69, 2015.

[4] M. Kok, J. D. Hol, and T. B. Schön, "Using inertial sensors for position and orientation estimation," *arXiv preprint arXiv:1704.06053*, 2017.

[5] Z. Li, L. Zhao, C. Qin, and Y. Wang, "Wifi/pdr integrated navigation with robustly constrained kalman filter," *Measurement Science and Technology*, vol. 31, no. 8, p. 084002, 2020.

[6] J. Chen, S. Song, and Z. Liu, "A pdr/wifi indoor navigation algorithm using the federated particle filter," *Electronics*, vol. 11, no. 20, p. 3387, 2022.

[7] M. Zhou, M. Dolgov, Y. Liu, and Y. Wang, "Wifi/pdr indoor integrated positioning system in a multi-floor environment," *EAI Endorsed Transactions on Cognitive Communications*, vol. 4, no. 14, 2018.

[8] Y. Kim, Y. Kyung, and H. Ko, "Indoor localization system with pdr and wifi complementary integration," in *2022 13th International Conference on Information and Communication Technology Convergence (ICTC)*. IEEE, 2022, pp. 1674–1676.

[9] X. Wang, T. Gao, J. Li, W. Guo, and D. Bai, "Wifi-pdr indoor fusion positioning based on ekf," in *2022 5th World Conference on Mechanical Engineering and Intelligent Manufacturing (WCMEIM)*. IEEE, 2022, pp. 933–937.

[10] A. Török, A. Nagy, L. Kováts, and P. Pach, "Drear-towards infrastructure-free indoor localization via dead-reckoning enhanced with activity recognition," in *2014 Eighth International Conference on Next Generation Mobile Apps, Services and Technologies*. IEEE, 2014, pp. 106–111.

[11] T. Liu, X. Zhang, Q. Li, and Z. Fang, "Modeling of structure landmark for indoor pedestrian localization," *IEEE Access*, vol. 7, pp. 15 654–15 668, 2019.

[12] H. Chen, F. Li, and Y. Wang, "Soundmark: Accurate indoor localization via peer-assisted dead reckoning," *IEEE Internet of Things Journal*, vol. 5, no. 6, pp. 4803–4815, 2018.

[13] X. Niu, L. Xie, J. Wang, H. Chen, D. Liu, and R. Chen, "Atlas: An activity-based indoor localization and semantic labeling mechanism for residences," *IEEE Internet of Things Journal*, vol. 7, no. 10, pp. 10 606–10 622, 2020.

[14] J. Sun, X. Yu, D. Liu, Y. Zhai, and C. Wang, "Research on indoor location technology based on the fusion of wifi and pdr," in *2020 13th International Conference on Intelligent Computation Technology and Automation (ICICTA)*. IEEE, 2020, pp. 416–419.

[15] M. Chattha and I. H. Naqvi, "Pilot: A precise imu based localization technique for smart phone users," in *2016 IEEE 84th Vehicular Technology Conference (VTC-Fall)*. IEEE, 2016, pp. 1–5.

[16] K. Kanagu, K. Tsubouchi, and N. Nishio, "Colorful pdr: Colorizing pdr with shopping context in walking," in *2017 International Conference on Indoor Positioning and Indoor Navigation (IPIN)*. IEEE, 2017, pp. 1–8.

[17] Q. Wang, H. Luo, L. Ye, A. Men, F. Zhao, Y. Huang, and C. Ou, "Personalized stride-length estimation based on active online learning," *IEEE Internet of Things Journal*, vol. 7, no. 6, pp. 4885–4897, 2020.

[18] F. Bo, J. Li, and W. Wang, "Mode-independent stride length estimation with imus in smartphones," *IEEE Sensors Journal*, vol. 22, no. 6, pp. 5824–5833, 2022.

[19] M. Vezočnik and M. B. Juric, "Adaptive inertial sensor-based step length estimation model," *Sensors*, vol. 22, no. 23, p. 9452, 2022.

[20] J. Kang, J. Lee, and D.-S. Eom, "Smartphone-based traveled distance estimation using individual walking patterns for indoor localization," *Sensors*, vol. 18, no. 9, p. 3149, 2018.

[21] Y. Yao, L. Pan, W. Fen, X. Xu, X. Liang, and X. Xu, "A robust step detection and stride length estimation for pedestrian dead reckoning using a smartphone," *IEEE Sensors Journal*, vol. 20, no. 17, pp. 9685–9697, 2020.

[22] C. Wu, F. Zhang, Y. Fan, and K. R. Liu, "Rf-based inertial measurement," in *Proceedings of the ACM Special Interest Group on Data Communication*, 2019, pp. 117–129.

[23] D. Wu, D. Zhang, C. Xu, Y. Wang, and H. Wang, "Widir: walking direction estimation using wireless signals," in *Proceedings of the 2016 ACM international joint conference on pervasive and ubiquitous computing*, 2016, pp. 351–362.

[24] Z. Wu, X. Pan, K. Fan, K. Liu, and Y. Xiang, "Device-free orientation detection based on csi and visibility graph," *IEEE Transactions on Systems, Man, and Cybernetics: Systems*, 2019.

[25] D. Halperin, W. Hu, A. Sheth, and D. Wetherall, "Tool release: Gathering 802.11 n traces with channel state information," *ACM SIGCOMM Computer Communication Review*, vol. 41, no. 1, pp. 53–53, 2011.

[26] F. Gringoli, M. Schulz, J. Link, and M. Hollick, "Free your csi: A channel state information extraction platform for modern wi-fi chipsets," in *Proceedings of the 13th International Workshop on Wireless Network Testbeds, Experimental Evaluation & Characterization*, 2019, pp. 21–28.

[27] "Ieee standard for information technology—telecommunications and information exchange between systems local and metropolitan area networks—specific requirements - part 11: Wireless lan medium access control (mac) and physical layer (phy) specifications," *IEEE Std 802.11-2016 (Revision of IEEE Std 802.11-2012)*, pp. 1–3534, 2016.

[28] C. Gentner, M. Ulmschneider, I. Kuehner, and A. Dammann, "Wifi-rtt indoor positioning," in *2020 IEEE/ION Position, Location and Navigation Symposium (PLANS)*. IEEE, 2020, pp. 1029–1035.